Exomer: a coat complex for transport of select membrane proteins from the trans-Golgi network to the plasma membrane in yeast

Chao-Wen Wang,[1,2] Susan Hamamoto,[1,2] Lelio Orci,[3] and Randy Schekman[1,2]

[1]Department of Molecular Cell Biology and [2]Howard Hughes Medical Institute, University of California, Berkeley, Berkeley, CA 94720
[3]Department of Cell Physiology and Metabolism, University Medical Center, 1121-Geneva 4, Switzerland

A yeast plasma membrane protein, Chs3p, transits to the mother–bud neck from a reservoir comprising the trans-Golgi network (TGN) and endosomal system. Two TGN/endosomal peripheral proteins, Chs5p and Chs6p, and three Chs6p paralogues form a complex that is required for the TGN to cell surface transport of Chs3p. The role of these peripheral proteins has not been clear, and we now provide evidence that they create a coat complex required for the capture of membrane proteins en route to the cell surface. Sec7p, a Golgi protein required for general membrane traffic and functioning as a nucleotide exchange factor for the guanosine triphosphate (GTP)–binding protein Arf1p, is required to recruit Chs5p to the TGN surface in vivo. Recombinant forms of Chs5p, Chs6p, and the Chs6p paralogues expressed in baculovirus form a complex of approximately 1 MD that binds synthetic liposomes in a reaction requiring acidic phospholipids, Arf1p, and the nonhydrolyzable GTPγS. The complex remains bound to liposomes centrifuged on a sucrose density gradient. Thin section electron microscopy reveals a spiky coat structure on liposomes incubated with the full complex, Arf1p, and GTPγS. We termed the novel coat exomer for its role in exocytosis from the TGN to the cell surface. Unlike other coats (e.g., coat protein complex I, II, and clathrin/adaptor protein complex), the exomer does not form buds or vesicles on liposomes.

Introduction

Vesicular trafficking provides a continuous exchange of proteins and lipids between membranes in a eukaryotic cell (for review see Rothman and Wieland, 1996; Schekman and Orci, 1996). Coat proteins are believed to confer much of the specificity associated with protein sorting into transport vesicles (Le Borgne and Hoflack, 1998a,b; Springer and Schekman, 1998). To date, three classes of coated vesicles have been identified: clathrin/adaptor-coated vesicles mainly involved in traffic between the TGN and the endosomes (Robinson, 1994); coat protein complex I (COPI), which is responsible for both retrograde transport from the Golgi back to the ER and intra-Golgi transport (Orci et al., 1997; Spang and Schekman, 1998); and COPII, which mediates anterograde transport from the ER to the Golgi apparatus (Bednarek et al., 1996; Schekman and Orci, 1996).

Coat assembly is initiated by activation of the ADP ribosylation factor (ARF) family of small G proteins (Arf1p and the closely related Sar1p) by which membrane-selective nucleotide exchange catalysts activate Arf1p or Sar1p for membrane attachment (Serafini et al., 1991; Donaldson et al., 1992; Palmer et al., 1993; Barlowe et al., 1994). Arf1p regulates the recruitment of COPI and most clathrin-containing coats, leading to membrane deformation into coated buds and vesicles. Likewise, COPII vesicles form when Sar1p-GTP recruits the inner coat complex (the Sec23/24p heterodimer) and the outer coat (the Sec13/31p heterotetramer; Matsuoka et al., 1998; Antonny et al., 2003; Lee et al., 2004).

Although coat proteins account for much of the vesicular traffic in a cell, no such involvement of coat proteins has been documented in the formation of vesicles or tubules that convey membrane and secretory proteins directly from the TGN to the cell surface. As an example of this limb of the secretory pathway, we have studied the transport of a cell wall biosynthetic enzyme, Chs3p (chitin synthase III), from the TGN/endosome membranes to the plasma membrane of the mother–bud junction in yeast. Chs3p is a multispanning transmembrane protein

Correspondence to Randy Schekman: schekman@berkeley.edu

Abbreviations used in this paper: ARF, ADP ribosylation factor; BFA, brefeldin A; COP, coat protein complex; FPLC, fast protein liquid chromatography; GEF, guanine nucleotide exchange factor; mArf1p, myristoylated Arf1p; NTA, nitrilotriacetic acid; PA, phosphatidic acid; PE, phosphatidylethanoamine.

The online version of this article contains supplemental material.

The Journal of Cell Biology, Vol. 174, No. 7, September 25, 2006 973–983
http://www.jcb.org/cgi/doi/10.1083/jcb.200605106

that is required for chitin ring formation during the G1 phase of the cell cycle and, subsequently, in lateral cell wall chitin synthesis (Shaw et al., 1991). Unlike other cell surface proteins, Chs3p export is regulated in response to cell cycle and stress signals (Shaw et al., 1991; Valdivia and Schekman, 2003). However, throughout the cell cycle, it is maintained in an intracellular reservoir by being recycled between the TGN and the early endosomes. This recycling is mediated by clathrin and an adaptor protein complex (AP-1). Chs5p and Chs6p are peripheral proteins that are required to transport Chs3p from the reservoir to the cell surface (Santos et al., 1997; Ziman et al., 1998). *chs5Δ* and *chs6Δ* mutants accumulate Chs3p in the TGN/endosome membranes, and the deletion of clathrin or subunits of AP-1 restores Chs3p traffic to the cell surface by some unknown bypass pathway (Valdivia et al., 2002). Thus, at least two mechanisms of traffic from the TGN/endosome membrane to the cell surface are possible for Chs3p. Each pathway involves an unexplored protein-sorting event that packages Chs3p into secretory vesicles that are delivered to the bud plasma membrane by the standard secretory pathway (Valdivia et al., 2002).

The Chs5 and Chs6 proteins are restricted to yeast and fungi, which may imply an organism-specific role such as the biosynthesis of yeast cell wall chitin. Yeast cells have three additional Chs6-like proteins (Bch1p [*YMR237W*], Bud7p, and Bch2p [*YKR027W*]), and their roles relative to Chs6p and the traffic of Chs3p are not yet understood (Satchatjate and Schekman, 2006; Trautwein et al., 2006). To pursue the role of Chs5p and Chs6p in the sorting and packaging of Chs3p, we have cloned and characterized the gene products, including the three paralogues of Chs6p. We have demonstrated that these Chs5 and Chs6 proteins are associated with each other in a complex that may make direct contact with Chs3p (Sanchatjate and Schekman, 2006). In this study, we identified Sec7p, a TGN-localized Arf1p nucleotide exchange factor that is required for the membrane association of Chs5p and regulating the interaction of Chs5p and Arf1p. We elucidated the biochemical requirements for membrane recruitment of a complex of Chs5p, Chs6p, and the Chs6p paralogues and describe a novel coat structure termed exomer, which forms when the complex is recruited to synthetic membranes in the presence of Arf1p and GTPγS.

Results

Chs5p membrane association is mediated by Sec7p

In a previous study, Santos and Snyder (2000) found Chs5p localized to puncta in cells marked by the TGN/endosome resident protein Kex2p. We confirmed the late Golgi localization of Chs5p-RFP by comparing its localization in vivo with Sec7p-GFP (late Golgi marker) and Anp1p-GFP (early Golgi marker) using double staining live cell imaging (Fig. S1, A–C; available at http://www.jcb.org/cgi/content/full/jcb.200605106/DC1). To determine whether this localization is perturbed when Golgi traffic is disrupted, we used a functional, integrated Chs5p-GFP to examine its localization in wild type and in cells defective in secretory protein traffic from the Golgi complex. In wild-type cells, Chs5p-GFP localized to spots dispersed within the cytoplasm, as was determined previously (Santos and Snyder, 2000), and this distribution was similar at 26 and 37°C.

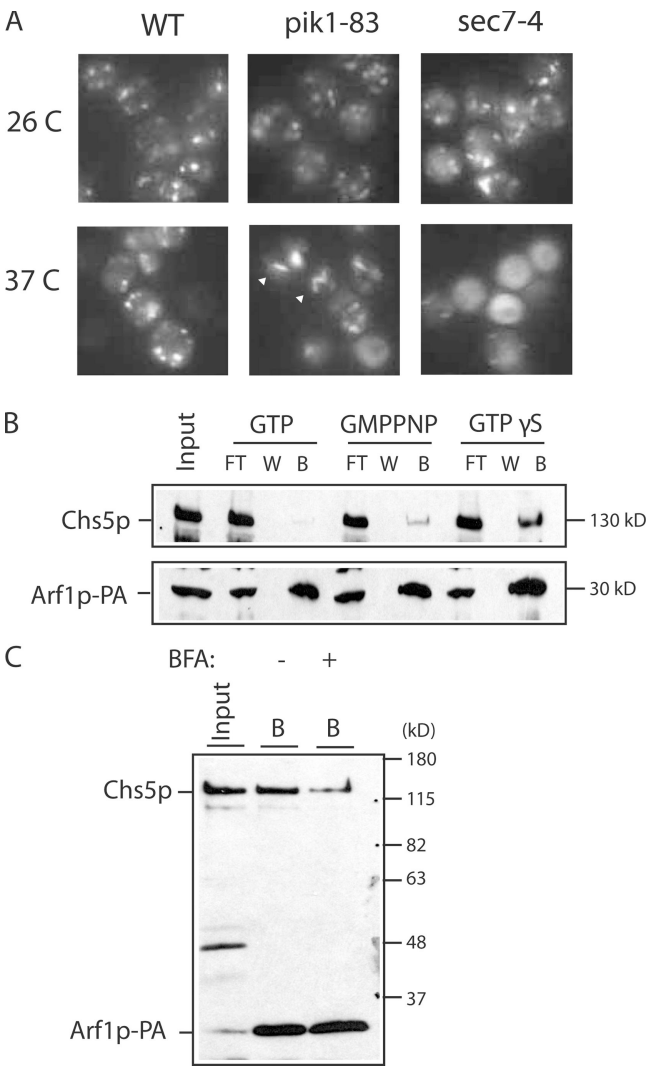

Figure 1. **Chs5p is regulated by a Sec7p- and Arf1p-dependent machinery.** (A) Chs5p-GFP localizes to Golgi membranes, and this association is Sec7p dependent. Wild-type (WT; CWY512), *pik1-83* (CWY559), and *sec7-4* (CWY612) cells that bear chromosomally tagged Chs5p-GFP were grown at 26°C to mid-log phase and either kept at 26°C or shifted to 37°C for 40 min for fluorescence microscopy. Arrowheads indicate exaggerated Golgi. (B) Chs5p interacts with Arf1p-PA. CWY506 cells harboring Arf1p-PA integrated at the chromosomal locus were harvested at mid-log phase as described in Materials and methods. A clear cell lysate (input) was distributed in aliquots and incubated with 0.5 mM GTP, GMP-PNP, or GTPγS for 10 min at 30°C. Arf1p–protein A was absorbed by IgG-coated Dynabeads at 4°C for 2 h. Beads were recovered using a magnet, and the unbound proteins were removed in the flow through (FT) followed by wash (W) steps. Protein remaining bound (B) to the beads was resuspended in buffer and analyzed by anti-Chs5p (also recognizes protein A [PA]) immunoblotting. (C) CWY506 was lysed as described in B followed by incubation with 0.5 mM GTPγS in the presence of buffer (−) or 2 μg/ml brefeldin A (BFA) at 30°C for 10 min. Samples were processed as in B except that only the bound (B) samples are shown.

We also expressed Chs5p-GFP in two temperature-sensitive mutants in which the secretory function of the Golgi apparatus can be altered. A temperature-sensitive allele of the *phosphatidylinositol 4-kinase* (*PIK1*) gene blocks protein secretion and accumulates exaggerated Golgi structures (Flanagan et al., 1993;

Hama et al., 1999; Walch-Solimena and Novick, 1999; Audhya et al., 2000). Similarly, temperature-sensitive alleles of *SEC7* arrest secretory traffic and accumulate large Golgi stacks at a restrictive temperature (Novick et al., 1980; Deitz et al., 2000). In the *pik1-83* strain at 37°C, Chs5p-GFP coalesced into large punctae, as was previously observed for the Golgi marker Och1p (Fig. 1 A; Strahl et al., 2005). In contrast, Chs5p-GFP dispersed in a diffuse pattern in *sec7-4* cells incubated at 37°C, although Chs5p-GFP localized normally at 26°C in both mutant strains (Fig. 1 A). The Golgi marker proteins Anp1p-RFP and Kex2p-GFP accumulated in exaggerated structures at 37°C in *sec7-4*, indicating that the Golgi membrane did not disperse (Fig. S1 D). Attempts to localize Chs6p-GFP were unsuccessful because the fluorescence of Chs6p-GFP was too weak for microscopy as a result of a low expression level (unpublished data).

SEC7 encodes a nucleotide exchange factor for Arf1p. One explanation for the difference between *pik1-83* and *sec7-4* is that the *sec7-4* mutation resides within the conserved Arf1 guanine nucleotide exchange factor (GEF) domain (Sec7 domain; Deitz et al., 2000). Thus, we considered the possibility that Chs5p was restricted to Golgi membranes through an interaction with activated Arf1p. To test this possibility, we created a strain harboring protein A fused to the C-terminal codon of the chromosomal copy of *ARF1*. A cytosol fraction obtained from this strain was incubated with GTP or one of two nonhydrolyzable analogues, GMP-PNP and GTPγS. Arf1p–protein A was recovered by binding to IgG-coated Dynabeads, and samples corresponding to the input, unbound wash fraction and bound (bead) materials were separated and evaluated by SDS-PAGE followed by Arf1p and Chs5p immunoblotting. A clear copurification of Chs5p with Arf1p was detected in incubations containing GTPγS and, to a lesser extent, with GMP-PNP (Fig. 1 B). Nucleotide hydrolysis in the GTP sample may explain the poor binding of Chs5p to Arf1p.

To further confirm the nucleotide-dependent interaction between Chs5p and Arf1p–protein A and to support the role of Sec7p in regulating this association, we next evaluated the recovery of bound Chs5p in incubations containing the ARF GEF inhibitor brefeldin A (BFA). We observed a reduction in the retention of Chs5p in an incubation containing GTPγS and 2 μg/ml BFA (Fig. 1 C). A similar effect of BFA in vivo has been reported by Trautwein et al. (2006). These experiments suggest that activated Arf1p-GTP, presumably by contact with Sec7p, recruits Chs5p to the Golgi membrane to initiate its role in the traffic of Chs3p.

Lipid-binding and Chs6 interaction domains of Chs5p

In addition to binding to activated Arf1p, Chs5p may interact by additional contact with the Golgi membranes. To determine whether Chs5p interacts with lipids, we expressed GST hybrid forms of Chs5p and Chs6p in *Escherichia coli*, and the purified GST hybrid proteins were probed for lipid interaction using an overlay assay on PIP strips. GST-Chs5p but not GST or GST-Chs6p showed significant interaction with most anionic lipids (unpublished data). A similar spectrum was seen with 6× His-tagged Chs5p expressed in yeast (unpublished data).

Fragments of Chs5p were fused to GST to define the region interacting with lipids (Fig. 2 A). The potential anionic lipid interaction domain was mapped to the C-terminal one third of Chs5p. This region may correspond to the C-terminal lysine-rich tail (Santos et al., 1997). Although the C-terminal domain may facilitate the membrane recruitment of Chs5p, it appears to be dispensable for chitin synthesis because a truncated version of *CHS5* corresponding to amino acid residues 1–401 complemented a *chs5Δ* strain based on the growth sensitivity of yeast cells making chitin to the chitin-binding dye calcofluor (unpublished data).

To understand the interaction between Chs5p and Chs6p, fragments of Chs5p used in the lipid-binding assay were evaluated for interaction with Chs6p using the yeast two-hybrid assay. Binding domain–Chs5p (aa 1–79) and binding domain–Chs5p (aa 1–260) showed two-hybrid interaction with activation

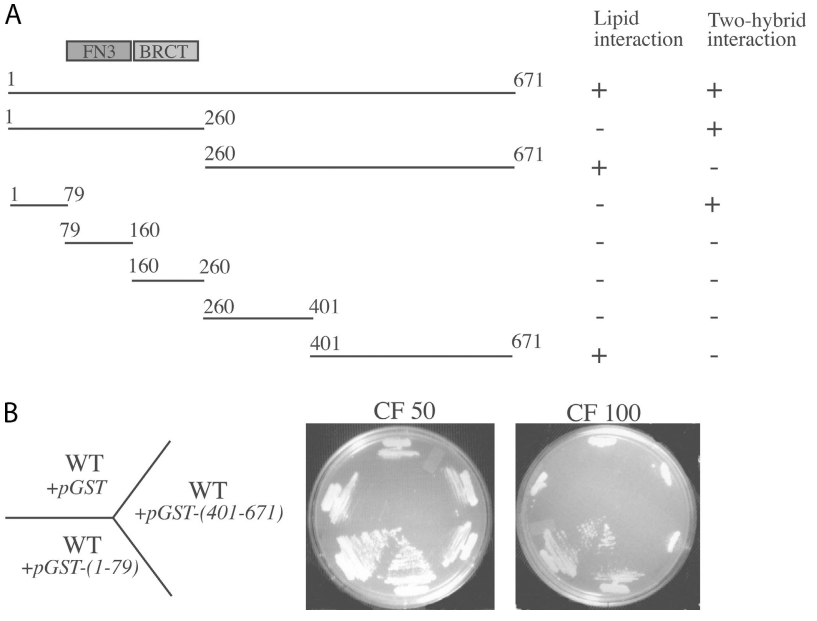

Figure 2. **Functional mapping of Chs5p.** (A) Mapping Chs5p lipid interaction and Chs6p interaction regions. Full-length Chs5p (aa 1–671) contains two motifs: FN3 (aa 79–160) and BRCT (aa 160–260). The fragments positive for lipid interaction are shown by a plus sign based on GST fusion constructs purified from *E. coli* that showed the lipid interaction profile on PIP strips (Echenlon). These fragments were also cloned into the yeast two-hybrid construct pGBD to test interaction with pGAD-Chs6. Growth on an SD-Leu-Ura-His plate is shown by a plus sign. (B) Wild-type (WT; SEY6210) cells harboring *GST*, *GST-Chs5 (aa 1–79)*, and *GST-Chs5 (aa 401–671)* cloned into pRS424 (2μ; tryptophan) were streaked on SD-Trp plates in addition to 50 (CF 50) or 100 μg/ml (CF 100) calcofluor. For each construct, two colonies were restreaked and examined on the plates.

domain–Chs6p (Fig. 2 A). These two domains (the lipid-binding domain within the C terminus of Chs5p and the Chs6 interaction domain within the N terminus of Chs5p) were compared by a competition assay evaluating their functional importance in chitin synthesis. The overexpression of GST hybrids containing the N-terminal domain of Chs5p interfered with Chs3p traffic as judged by the calcofluor growth test, whereas a GST hybrid containing the C-terminal domain of Chs5p did not impair chitin synthesis (Fig. 2 B). Thus, the interaction of Chs5p and Chs6p may be crucial for the transport of Chs3p.

A purified recombinant complex of Chs5p, Chs6p, and Chs6 paralogues

To further investigate the role of activated Arf1p in Chs5p membrane recruitment (Fig. 1), we sought to isolate the Chs5p- and Chs6p-containing complex (Fig. 2) for functional tests. Efforts to express the proteins in stable oligomeric forms in *E. coli* and yeast resulted in poor yields. However, expression in baculovirus proved more reliable. We created baculovirus vectors containing N-terminally 6× His-tagged Chs5p and untagged versions of one or more copies of Chs6p and its paralogues (Bch1p, Bud7p, and Bch2p; Fig. 3 A). Recent evidence has suggested that Chs5p interacts with Chs6p and each of the Chs6 paralogues and that complexes include more than one copy of Chs6p and its paralogues (Sanchatjate and Schekman, 2006; Trautwein et. al., 2006). The baculovirus system allowed us to evaluate complex formation by coexpressing multiple combinations of these recombinant Chs5p and Chs6p proteins. Consistent with previous observations (Sanchatjate and Schekman, 2006; Trautwein et. al., 2006), we found that Chs5p copurified with each Chs6p or its paralogue when the two were coexpressed and that multiple paralogues of Chs6p copurified with Chs5p from cells expressing two, three, or all Chs6p and Chs6p paralogues (Fig. 3 A and not depicted).

In most cases, the apparent abundance of Chs5p, based on Sypro red staining intensity, approximated the abundance of the sum of the Chs6 and Chs6p paralogues. Bch2p was a notable exception, perhaps because of a lower virus titer. Infection with a larger Bch2 baculovirus stock increased the abundance of this species in the isolated Chs5p complex (unpublished data). The ratios of the Chs6p species in the complex differed from those detected in the complex isolated from wild-type yeast cells

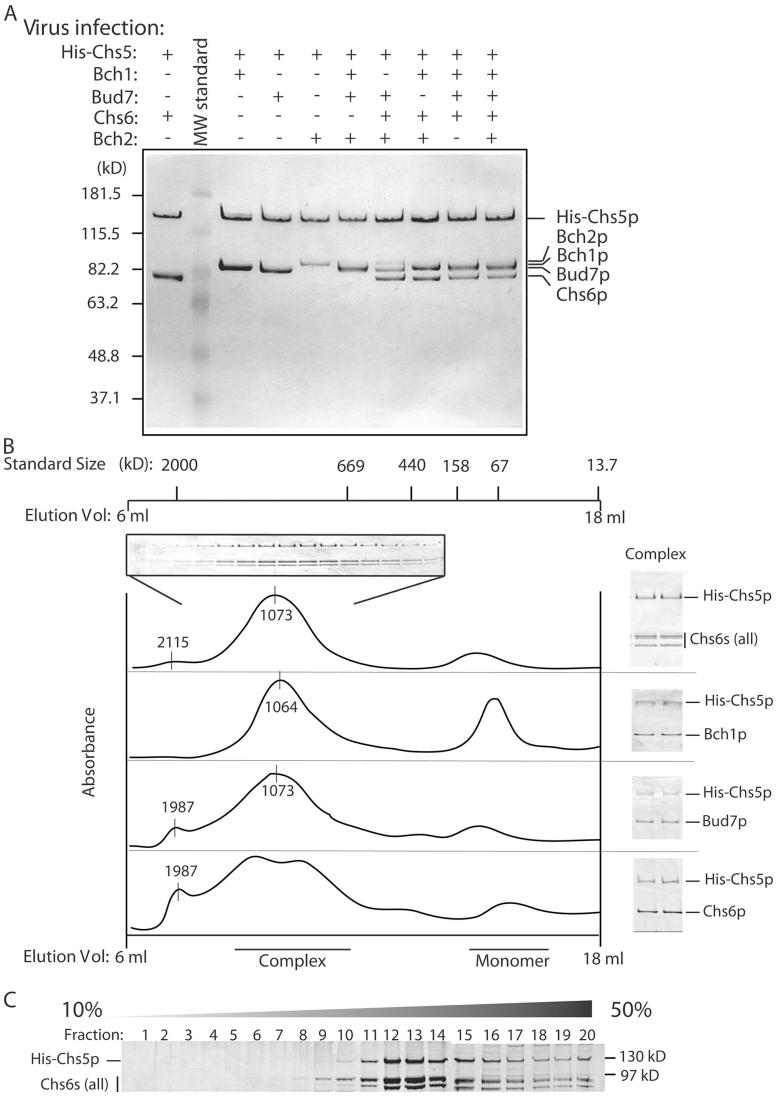

Figure 3. **Purification and characterization of the Chs5p and Chs6p protein complexes.** (A) Chs5p and all Chs6-like proteins were purified as complexes. Amplified baculovirus stocks were inoculated (+) or not inoculated (−) into the insect culture cell line Sf-9. Cultures were harvested after 4 d postinoculation, and proteins were purified on a Ni-NTA column (for binding to 6× His-tagged Chs5p). Purified proteins were examined by SDS-PAGE followed by Coomassie blue staining. MW, mol wt. (B) Protein complexes purified on Ni-NTA were size fractionated on a Superose 6 FPLC column. Elution during 6–18 ml is shown, and the localization of mol wt standards is indicated. Peak fractions of the complex (size as indicated) were analyzed by SDS-PAGE and Sypro red staining. As examined on gels, His-Chs5p and Chs6p-like proteins such as Bch1p, Bud7p, and Chs6p are found together in the ~1-MD fractions. (C) The purified Chs5–Chs6[all] complex was analyzed by a 10–50% sucrose gradient. A total of 20 × 100-μl fractions were collected from the top, and proteins were analyzed by SDS-PAGE and Sypro red staining. Gels were visualized using a Typhoon imager.

(Sanchatjate and Schekman, 2006), probably reflecting the different level of *CHS* gene expression in these circumstances. The recombinant expression of Chs6p and its paralogues without Chs5p also resulted in complexes including Chs6p and one or more Chs6p paralogues (unpublished data).

Affinity-purified complexes were evaluated by gel filtration on a Superose 6 fast protein liquid chromatography (FPLC) column to determine the size and composition of the complex. Complex isolated from cells expressing Chs5p and all four Chs6p and its paralogues (Chs5–Chs6[all]) fractionated at a position consistent with a size slightly >1 MD with coincident chromatography of the most abundant Chs6p species (Fig. 3 B). Similar patterns of filtration were seen with complexes containing only one Chs6p paralogue, although a complex of Chs5p and Chs6p fractionated somewhat heterogeneously. An independent method of separation, velocity sedimentation on a sucrose density gradient, confirmed that Chs5p, Chs6p, and Chs6p paralogues (Chs5–Chs6[all]) were present in a large complex (Fig. 3 C). This pattern of cosedimentation was not altered in the Chs5–Chs6[all] samples treated with 3 M urea, 1% Triton X-100, or 1 M KCl (unpublished data). Overall, recombinant Chs5p, Chs6p, and Chs6p paralogues, like those isolated from wild-type yeast cells, appear to be self-organized into a large and stable complex.

Myristoylated Arf1p-GTPγS recruits the Chs5–Chs6[all] complex to liposomes

Because genetic evidence suggests that more than just one of the Chs6p and its paralogues is required for traffic of Chs3p to the cell surface (Sanchatjate and Schekman, 2006; Trautwein et al., 2006), we used the complex including Chs5p, Chs6p, and three Chs6 paralogues (Chs5–Chs6[all]) to evaluate the role of activated Arf1p in membrane recruitment. Recombinant myristoylated Arf1p (mArf1p; Q71L; GTPase deficient) was purified from *E. coli* and mixed with GTPγS and liposomes formulated with synthetic phospholipids with various levels of selected acidic phospholipids (Fig. 2 A; Spang et al., 1998). EDTA was included to stimulate spontaneous GTP/GDP exchange on Arf1p (Antonny et al., 1997). After 1 h at 30°C, $MgCl_2$ was added to stabilize Arf1-GTPγS, and the samples were supplemented with Chs5–Chs6[all] and incubated for a further 10 min at 22°C. For each liposome formulation, three samples were prepared: complete, without Arf1p, and without GTPγS. Liposomes and bound proteins were separated from unbound materials by flotation sedimentation on a sucrose density shelf. Fig. 4 A documents the recovery of proteins bound to liposomes, and Fig. 4 B displays a quantitative representation of proteins recovered in the floated fractions. In most samples, Arf1p bound to liposomes in the presence or absence of GTPγS. However, recruitment of the Chs5–Chs6[all] complex was optimum in incubations that contained Arf1p and GTPγS.

Certain liposome formulations (e.g., phosphatidylcholine/phosphatidylethanoamine [PE]/phosphatidylserine/phosphatidic acid [PA] with a high concentration of PI(4)P or phosphatidylinositol-4,5-bisphosphate) recruited Chs5–Chs6[all] in the absence of Arf1p or GTPγS (Fig. 4, A and B). Other formulations (e.g., major-minor mix optimized for COPII assembly; Matsuoka et. al., 1998) displayed a substantial GTPγS requirement for recruitment of the Chs5–Chs6[all] complex. From these results, we conclude that Arf1p binds directly to the Chs5–Chs6[all] complex and facilitates the association of the complex with liposomes, particularly with certain formulations containing one or more of several acidic phospholipids.

The major-minor mix formulation, which was optimized for the recruitment of activated Sar1p and COPII to liposomes (Matsuoka et al., 1998) and which also works well for the recruitment of activated Arf1p and coatomer (COPI; Spang, et al., 1998), was reexamined for wild-type Arf1p and Chs5–Chs6[all] assembly in the presence of various nucleotides. Fig. 4 C shows a substantial dependence on GTPγS (or GMP-PNP), with much less of the complex recruited in the presence of GDP or GTP. GTP hydrolysis during recruitment and liposome sedimentation may explain the failure to retain comparable amounts of the Chs5–Chs6[all] complex on liposomes incubated with Arf1p-GTP. Likewise, a Golgi-enriched membrane fraction incubated with the Chs5–Chs6[all] complex confirmed that the binding of Chs5–Chs6[all] in a reaction was stimulated by GTPγS (unpublished data).

We next compared recruitment of the Chs5–Chs6[all] complex to the other subcomplexes formed with Chs5p, Chs6p, or fewer paralogues of Chs6p (Fig. 4 D). Chs5p alone was very inefficiently recruited to major-minor liposomes. Combinations including one paralogue were recruited in a manner largely independent of GTPγS. However, two paralogues known to be important in Chs3p traffic (Chs6p and Bch1p) were recruited to membranes in an Arf1p-GTPγS–dependent manner comparable with Chs5–Chs6[all] (Fig. 4 D).

Stoichiometric recruitment of the Chs5–Chs6[all] complex to liposomes

To provide evidence that the recruitment is under control by a specific, regulated process, we varied the concentration of Arf1-GTPγS and the Chs5–Chs6[all] complex and the time of incubation to discover the optimum conditions of assembly on major-minor mix liposomes. Two-stage recruitment assays were performed. Liposomes were incubated with ~1 μM mArf1p and GTPγS in a first-stage binding reaction as in Fig. 4 and were mixed with the Chs5–Chs6[all] complex for 15 min at 22°C. Membrane-bound protein complexes were collected by flotation on a step sucrose cushion, and the protein content was measured by Sypro red staining of gels (Fig. 5 A). Chs5–Chs6[all] complex binding to liposomes was saturated at ~0.5 μM in this experiment. Conversely, at a fixed Chs5–Chs6[all] concentration of ~0.8 μM, Arf1p binding increased nonsaturably (Fig. 5 B, ii), whereas binding of the Chs5–Chs6[all] complex appeared to approach saturation at around 1.5 μM Arf1p (Fig. 5 B, i). Excess bound Arf1p may not be functional or accessible to the Chs5–Chs6[all] complex. Titration at the low range of Arf1p, where the linear membrane association of Arf1p and Chs5p was shown (Fig. 5 B, iii), indicated an ~7.5:1 molar stoichiometry of the Arf1/Chs5–Chs6[all] complex, reflecting either a substantial fraction of bound Arf1p that is not accessible to the Chs5–Chs6[all] complex or incomplete density gradient recovery of Chs5–Chs6[all] compared with activated Arf1p bound to liposomes.

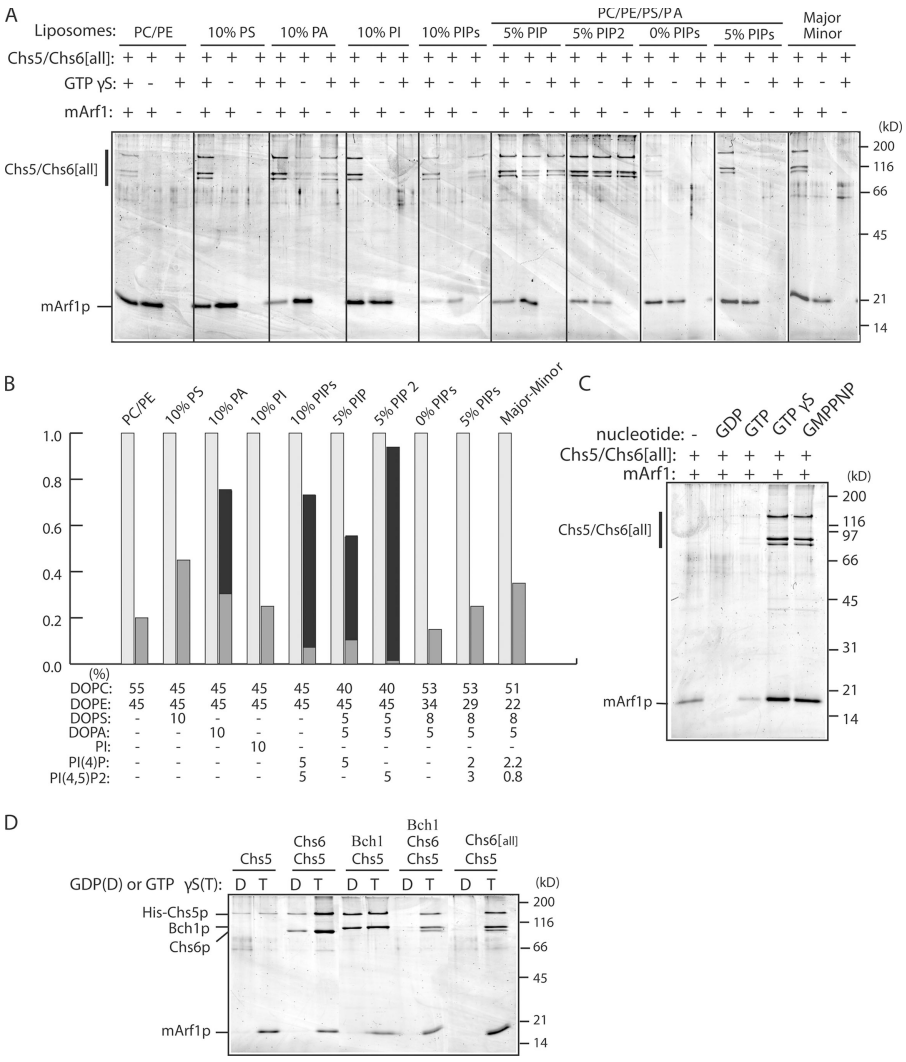

Figure 4. **Recruitment of the Chs5–Chs6[all] complex by mArf1p.** (A) Liposomes composed of various phospholipid formulations were tested for recruitment of the Chs5–Chs6[all] complex in the presence of GTPγS alone, mArf1p(Q71L) alone, or mArf1p(Q71L) and GTPγS. Liposomes were floated through a step sucrose gradient as described in Materials and methods. Liposome-bound proteins were analyzed by SDS-PAGE followed by Sypro red staining. Gels were visualized using a Typhoon imager. (B) Comparison of binding as shown in A. mArf1p recovery from different liposome formulations as shown in A was set at 100% (light gray bar), relative recoveries of the His-Chs5p amount (wt/wt) are compared (gray bar), and the amount of His-Chs5p floated in the absence of mArf1p was subtracted (black bar) from the gray bar. The y axis measures the relative binding index. (C) Standard recruitment assay. Major-minor liposomes were incubated with 1 μM mArf1p in the presence of buffer (−), 0.1 mM GDP, GTP, GTPγS, or GMP-PNP at 30°C for 1 h in a chelating condition used to trigger nucleotide exchange. 0.5 μM Chs5–Chs6[all] complex was tested for binding as described in Materials and methods. Floated proteins were examined by Sypro red staining. (D) The same mArf1p exchange conditions were performed as in C, but different proteins or protein complexes were tested for their association with mArf1p in the presence of 0.1 mM GDP (D) or GTPγS (T). PC, phosphatidylcholine; PS, phosphatidylserine; PI, phosphatidylinositol.

The relationship of Arf1p exchange and Chs5–Chs6[all] recruitment in a reaction was evaluated in a time course experiment. Protein binding to liposomes was conducted with Arf1p at approximately the maximum Chs5–Chs6[all] ratio achieved in the titration experiment in Fig. 5 A. Incubations included EDTA to promote Arf1p nucleotide exchange. Samples were collected at the indicated times at 30°C, mixed with $MgCl_2$, and chilled on ice for the duration. The kinetics of binding paralleled the rate of EDTA-stimulated Arf1p nucleotide exchange as measured by the change in tryptophan fluorescence of activated Arf1p (Fig. 5 C and not depicted; Antonny et al., 1997). These results support our conclusion that GTPγS-activated Arf1p recruits the Chs5–Chs6[all] complex to the membrane.

Chs5–Chs6[all] complex forms a coated surface on liposomes

Given the similarity between the Chs5–Chs6[all] complex and the COPs (coatomer and COPII) in regard to Arf1p-GTPγS (or Sar1p–GMP-PNP)–dependent recruitment to liposomes, we examined the influence of this assembly on the buoyant density of liposomes. COPII proteins that assemble on liposomes in the presence of Sar1p–GMP-PNP cause membranes to shift to a higher buoyant density, reflecting the formation of protein-coated surfaces and synthetic COPII vesicles (Matsuoka et al., 1998). We formulated major-minor mix liposomes with Texas red–PE and conducted assembly incubations for the complete reaction containing Arf1-GTPγS and Chs5–Chs6[all] as described above. Samples were applied to a 10–50% linear sucrose gradient and centrifuged to equilibrium for 16 h at 4°C. In control incubations, in samples of liposomes incubated with the Chs5–Chs6[all] complex without Arf1p or GTPγS or liposomes incubated with Arf1p and GTPγS alone (unpublished data), fluorescent lipid peaked at the top of the gradient (fraction 1). In a complete reaction, most of the fluorescent lipids and Arf1p sedimented into the gradient but remained in the low density liposome fractions (Fig. 6, C and D; fractions 2–8), whereas most of the unbound Chs5–Chs6[all] complex sedimented to a high density with no apparent lipid cofractionation (Fig. 6, B and D). Chs proteins and Arf1p were detected in fractions 2–8 but not in a sample of Chs5–Chs6[all] incubated with liposomes in the absence of Arf1p (Fig. 6, B and C). Thus, at least some liposome-bound Chs proteins may coat membranes sufficiently to influence membrane buoyant density.

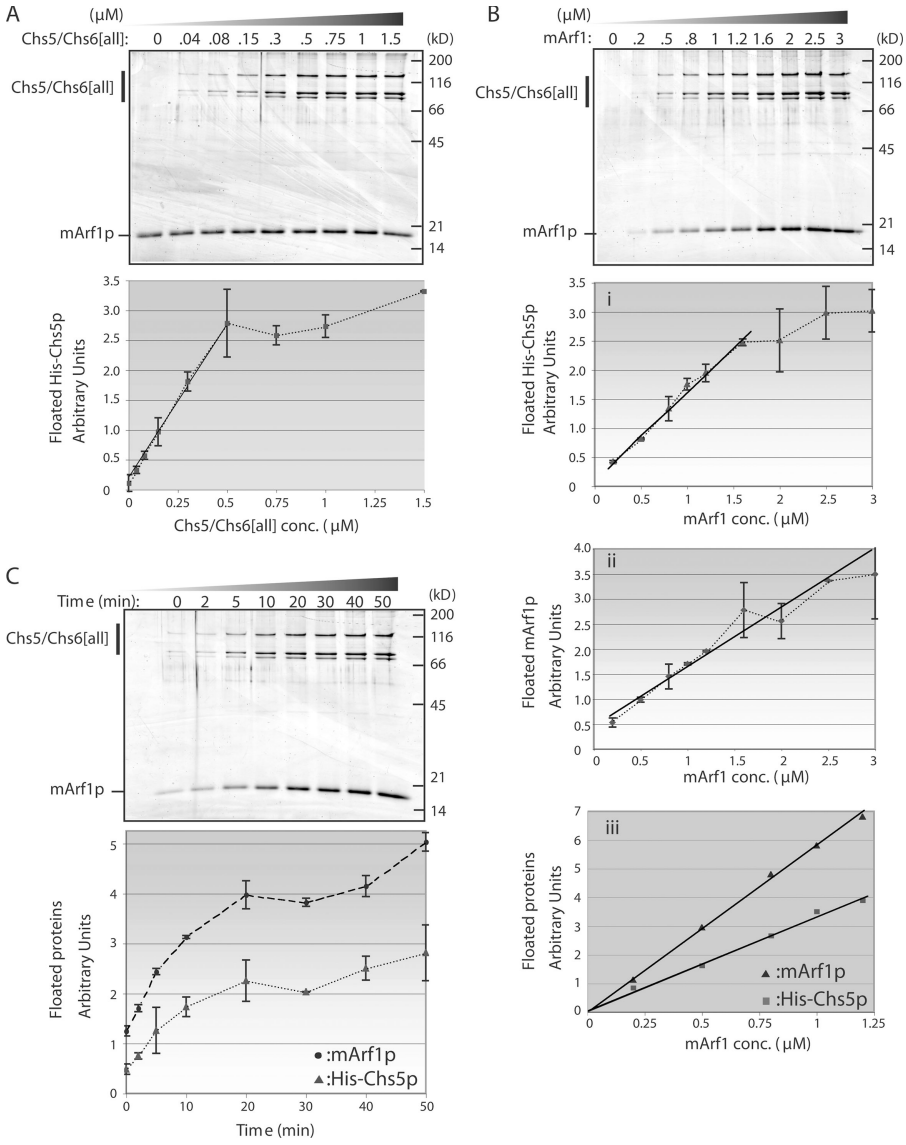

Figure 5. **Recruitment of the Chs5–Chs6[all] complex via mArf1p in the presence of GTPγS is a saturable process.** (A) Titration of the Chs5–Chs6[all] complex. 1 μM mArf1p incubated with GTPγS and various concentrations of the Chs5–Chs6[all] complex at room temperature for 15 min. Recruitment was determined by a step flotation gradient as described in Materials and methods. Sypro red staining of one experiment is shown, and quantitative results from several experiments are plotted below. (B) Titration of mArf1p with a fixed amount of the Chs5–Chs6[all] complex. Various amounts of mArf1p were incubated with GTPγS for 1 h at 30 min. 0.8 μM of a fixed concentration of the Chs5–Chs6[all] complex was then tested for binding at room temperature for 15 min. Recruitments were determined by a step flotation gradient as described in Materials and methods. Sypro red staining of one experiment is shown, and quantitative results from several experiments are plotted below. (i and ii) The membrane-associated His-Chs5p (i) and mArf1p (ii) are quantified. (iii) The membrane-associated His-Chs5p versus mArf1p (wt/wt) before the saturation concentration is quantified. (C) Recruitment time course experiment. 1 μM mArf1p and 0.5 μM Chs5–Chs6[all] complex were mixed at t = 0. Reactions were incubated at 30°C and stopped at the indicated times. Membrane association of His-Chs5p versus mArf1p (wt/wt) was determined by a step flotation gradient as described in Materials and methods. Sypro red staining of one experiment is shown, and quantitative results from several experiments are plotted below. Error bars represent SD.

The unambiguous assignment of a membrane coat requires inspection by thin section electron microscopy. Samples were prepared from a complete incubation (Fig. 7 A), an incubation of liposomes and Arf1p-GTPγS alone (Fig. 7 C), and an incubation with Arf1p, Chs5–Chs6[all] complex, and GDP (Fig. 7 B). A spiky coat appeared uniformly distributed along the surface of liposomes incubated under conditions in which the Chs5–Chs6[all] complex binds to the membrane but not in the control conditions. Although some membrane profiles appeared elongated, no coated buds or small coated vesicles were evident. Thus, the Chs5–Chs6[all] complex, which we now call exomer, appears to form coats on the membrane. However, unlike the COPs, exomer by itself does not deform membranes to induce the formation of buds and transport vesicles.

Discussion

Vesicular traffic in several limbs of the secretory pathway is initiated by the GTP-binding protein-dependent recruitment of coat proteins that sequester cargo molecules in a bud and pinch the membrane to form a transport vesicle. Clathrin, COPI, and COPII are well-known examples of this seemingly general feature (for review see Rothman and Wieland, 1996; Schekman and Orci, 1996). However, one clear gap in our knowledge concerns the mechanism of sorting and transport of membrane and secretory proteins from the TGN to the cell surface. Although some proteins use clathrin to traverse the endosome en route to the cell surface (Ang et al., 2004), others do not, and, until now, the general view has been that the direct path out of the TGN may involve tubular carriers formed without the intervention of coat proteins. Some regulatory proteins control the formation of transport carriers at the TGN by modulating lipid composition (for example, activation of phospholipase D by protein kinase C; Simon et al., 1996). Other proteins, such as FAPPs (four-phosphate adaptor proteins), are phosphoinositide-binding proteins that are found associated with TGN carriers and also interact with Arf1p (Godi et al., 2004). Protein kinase D is recruited to the TGN through interaction with diacylglycerol and

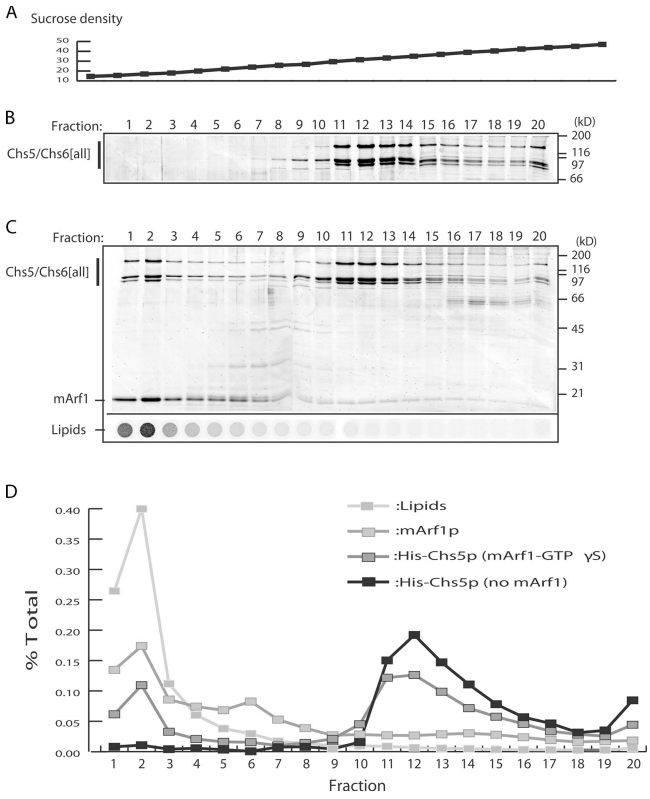

Figure 6. **Enrichment of coated membrane on a sucrose density gradient.** (A) Sucrose density index for the gradient centrifuged at 4°C for 16 h at 100,000 *g* in a TLS55 rotor. (B) Distribution of the Chs5–Chs6[all] complex (11–20) alone. (C) Cofractionation of lipids, mArf1p, and the Chs5p–Chs6[all] complex in the lighter fractions (1–10). (D) Quantification of the distribution in B and C.

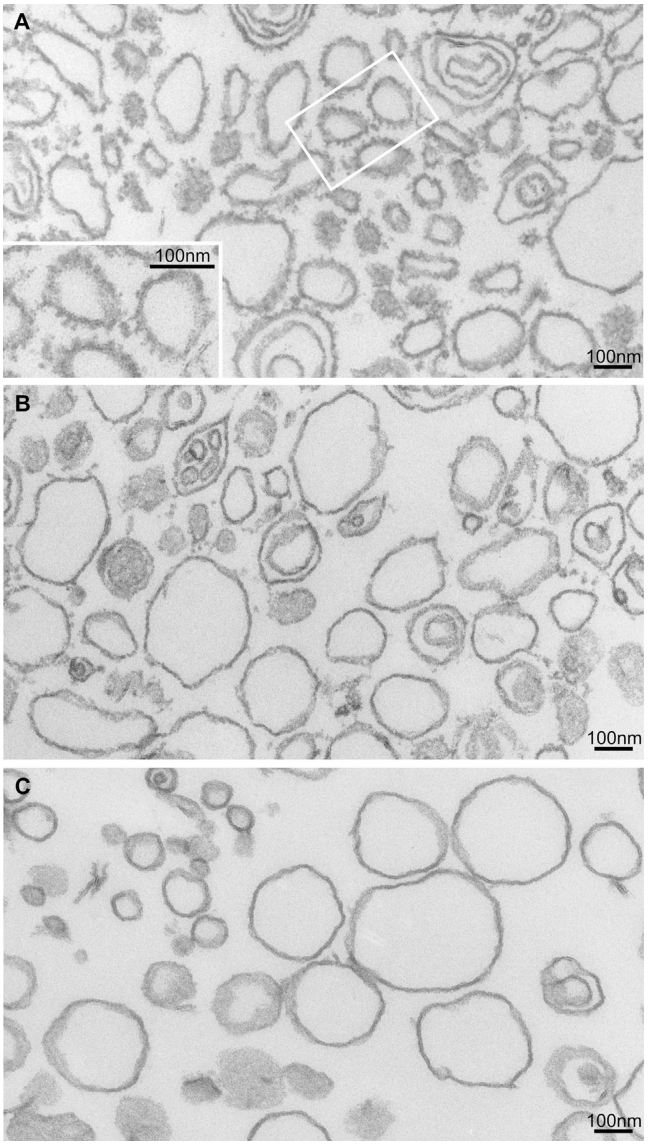

Figure 7. **Coating of the Chs5–Chs6[all] complex on liposomes.** (A) Major-minor liposomes were incubated with mArf1p and GTPγS at 30°C for 1 h, and the Chs5–Chs6[all] complex was then added and incubated at room temperature for 15 min followed by fixation for thin section electron microscopy. An extensive coating on liposomes can be seen as spikes formed by patches. The inset is a higher magnification view of the boxed area. (B) Major-minor liposomes were incubated with mArf1p-GDP for 1 h at 30°C, and the Chs5–Chs6[all] complex was added at room temperature for 15 min. (C) Major-minor liposomes were incubated with mArf1p-GTPγS alone at 1 h at 30°C, and buffer was added at room temperature for 15 min.

is subsequently activated by phosphorylation to promote carrier fission (Liljedahl et al., 2001).

We have investigated traffic of the plasma membrane enzyme that makes the chitin ring at the mother–bud junction in growing yeast cells. This protein, Chs3p, has an interesting itinerary and set of genetic requirements for its traffic that are somewhat distinct from the requirements of other cell surface proteins. Specifically, the action of two peripheral membrane proteins, Chs5p and Chs6p, suggest a special machinery to convey Chs3p from the TGN to the cell surface (Valdivia et al., 2002). Chs5p and Chs6p form subunits of a complex, including one or more additional Chs6p paralogues that also facilitate the traffic of Chs3p (Sanchatjate and Schekman, 2006; Trautwein et. al., 2006). Chs5p is required for the transport of at least two other proteins in addition to Chs3p, one of which, Fus1p, a cell surface protein required for yeast cell fusion, does not depend on Chs6p (Santos and Snyder, 2003). By analogy to the paralogues of Sec24p that form dimers with Sec23p in the COPII coat (Shimoni et al., 2000), we propose that Chs5p, Chs6p, and its paralogues may recognize distinct sets of membrane cargo proteins at the TGN for packaging into mature secretory vesicles.

Our strategy has been to identify conditions that promote the recruitment of Chs5p and Chs6p to the TGN/endosomal membrane and then to reconstruct this interaction with synthetic membranes. Two lines of evidence support a role for activated Arf1p in Chs5p–Chs6p assembly at the TGN. Trautwein et al. (2006) found that Arf1p-GTPγS binds Chs5p and Chs6p in a crude lysate of yeast. In vivo, nucleotide exchange on Arf1p is promoted by several proteins sharing a GEF domain that was first identified in a peripheral Golgi protein, Sec7p, which is required for secretory traffic within the Golgi complex. Mutations within the Sec7 GEF domain block traffic of all or most secretory proteins and disperse Chs5p from its normal punctate TGN/endosomal localization (Fig. 1 A). BFA blocks GEF activity and reduces the recruitment of Chs5p to immobilized

Arf1p-GTPγS (Fig. 1 C). Arf1p-GTP may tether Chs5p to membrane much as it does for coatomer in COPI vesicle formation and adaptor proteins (AP-1 and -2) for clathrin-coated vesicles and as Sar1p-GTP does for Sec23p–Sec24p in COPII coat assembly.

Coat recruitment and assembly on artificial membranes is stimulated by acidic phospholipids. Recombinant Chs5p interacts with Chs6p and with a variety of acidic phospholipids (Figs. 2 and 4). Recombinant complex expressed in baculovirus-infected Sf-9 cells as combinations of Chs5p, Chs6p, and one or more of the Chs6p paralogues fractionates as an ∼1-MD complex that binds to artificial membranes in an Arf1-GTPγS (or GMP-PNP)–dependent manner (Fig. 4). Optimal interaction occurs on liposomes that are similar in composition to those formulated for the recruitment and assembly of the COPII and I coats (Matsuoka et al., 1998; Spang et al., 1998). Complexes formed with binary combinations of Chs5p and Chs6p or one other Chs6p paralogue are somewhat less strictly dependent on Arf1p-GTPγS for membrane recruitment. Thus, we suggest that the native mixed complex (i.e., Chs5–Chs6[all]) is the likely form recruited to TGN membranes in vivo.

The Chs5–Chs6[all] complex binds to and perturbs the density of liposome membranes (Fig. 6). Thin section microscopy of fixed, membrane-bound complex reveals an electron-dense coat whose morphology is quite distinct from that seen for other coating complexes associated with cargo traffic (Fig. 7). Unlike COPII and I, which assemble onto and vesiculate artificial liposomes, the Chs5–Chs6[all] coat forms a spiky structure but does not pinch the membrane into buds and small vesicles. We propose to call the Chs coat the exomer to reflect its role in the exocytosis of Chs3p and select additional proteins. Although this coat also traffics a subset of other cargo proteins, the subunits are dispensable for normal cell viability, and the *CHS5* and *CHS6* genes are largely restricted to fungi that make chitin. It seems likely that other coats of similarly restricted roles will be uncovered in yeast and in other organisms, but the null phenotype of such coat subunits may not be nearly as dramatic as one normally associates with a general block in secretion.

The absence of coated buds and small vesicles in the preparation of exomer-coated liposomes suggests that other factors cooperate with the exomer to convey cargo proteins out of the TGN donor compartment. Chs3p interacts with Chs5p–Chs6p (Sanchatjate and Schekman, 2006; Trautwein et al., 2006), and it is possible that cargo-coat contact may promote the shape change that accompanies vesicle morphogenesis. Alternatively or in addition, the exomer may engage elements of the cytoskeleton, perhaps actin directly, to draw cargo molecules into tubules much as has been shown for cooperative interaction of clathrin, actin, and the Arp2/3 complex in cell surface invagination and endocytosis in yeast (Kaksonen et al., 2003, 2005). Indeed, genetic studies link Chs5p and Chs6p to elements of the cytoskeleton (Tong et al., 2004; Lesage et al., 2005). A biochemical reconstitution approach with exomer, liposomes, and cytoskeletal proteins may now be used in an effort to recapitulate the formation of more fully developed TGN to cell surface traffic intermediates.

Materials and methods

Yeast strains and materials

GFP was integrated at the C-terminal codon of the *CHS5* locus by a PCR-based one-step transformation procedure (Longtine et al., 1998). Primers for C-terminal GFP integration were 5′-AAGAAGAATAAGAAGAATAAGAAGAAAGGGAAAAAGAAACGGATCCCCGGGTTAATTAA and 3′-ATAAAAAATAGATTATATTTGCTGAGGGATTCTCAGTCGGAATTCGAGCTCGTTTAAAC. A similar approach was applied to generate the Arf1-PA and *chs5Δ* strains. Primers for C-terminal Arf1 integration were 5′-GGTTTGGAATGGTTAAGTAACAGTTTGAAAAACTAAACTCGGATCCCCGGGTTAATTAAand 3′-CTTTATGTTTCATTTAGTTTATACAAGCGTATTTGATCCGAATTCGAGCTCGTTTAAAC. Deletion primers to generate *chs5Δ* were 5′-GTCTTCAGTTGATGTACTGTTAACAGTAGGTAAGTTGGACGGATCCCCGGGTTAATTAA and 3′-ATAAAAAATAGATTATATTTGCTGAGGGATTCTCAGTCGGAATTCGAGCTCGTTTAAAC.

Yeast strains used in this study include the following: SEY6210 (*MATα, leu2-3, ura3-52, his3-Δ200, lys2-801, trp-Δ901, suc2-Δ9*), CWY512 (*Chs5-GFP::HIS3 SEY6210*), CWY559 (*MATa pik1-83:TRP1 ade2-101och his3-200 leu2-1 lys2-801a trp1-d ura3-52, Chs5-GFP::HIS3, pRS412*), CWY612 (*MATa ura3-1 leu2-3112 trp1-Δ1 his3-11,15 sec7-4, Chs5-GFP::KAN*), CWY506 (*Arf1-PA::HIS SEY6210*), CWY624 (*chs5Δ::LEU2 SEY6210*), and PJ69-4A (*MATα, trp1-901, leu2-3, 112, ura3-52, his3-200, gal4Δ, gal80Δ, LYS2::GAL1-HIS3, GAL2-ADE2, met2::GAL7-lacZ*).

All chemical reagents were purchased from Sigma-Aldrich unless specified. Lipids were obtained from Avanti Polar Lipids, Inc., and PIP strips were purchased from Echenlon. Sypro red protein staining dye was purchased from Invitrogen. Complete protease inhibitor cocktail was obtained from Roche Molecular Biochemicals. *E. coli* BL21 (DE3) coexpressing yeast *N*-myristoltransferase and Arf1 (wild type and Q71L) were provided by R. Kahn (Emory University, Atlanta, GA). Anti-Chs5 antiserum was described previously (Sanchatjate and Schekman, 2006). Anti-GST antibody was purchased from Santa Cruz Biotechnology, Inc. DH10Bac Competent cells and the Bac-to-Bac baculovirus expression system were purchased from Invitrogen. Glutathione-Sepharose fast flow, pGEX vector, and the Superose 6 gel filtration column were obtained from GE Healthcare. Dynabead M-500 subcellular was purchased from Dynal.

Protein purification

GST, GST-Chs5, GST-Chs6, and other GST-Chs5 fragments shown in Fig. 1 B were constructed in the pGEX vector (GE Healthcare), and proteins were purified from *E. coli* BL21. In brief, 1 L of cell culture was grown to A_{600} = 0.5–1.0 followed by 200 μM IPTG induction for 3 h at 22°C. Cells were resuspended in 20 ml PBS buffer, lysed by sonication, and centrifuged at 12,000 rpm for 10 min. The clear cell lysate was incubated with 5 ml glutathione-Sepharose (prewashed by PBS) at 4°C for 3 h. Beads and adsorbed proteins were poured into a column, and 3 × 30 ml PBS aliquots were applied to the column to remove nonspecific material. Bound proteins were eluted with 12 ml PBS + 10 mM of reduced glutathione. For the lipid-protein overlay assay, we adjusted purified proteins to 150 μg/ml and followed the procedures recommended by the manufacturer (Echelon).

mArf1p was purified from an *E. coli* BL21 (DE3) strain that coexpressed yeast *N*-myristoyltransferase and either wild-type or dominant-activated (Q71L) Arf1p. The purification procedures have been published previously (Randazzo et al., 1992), except a Sephacryl S-100 column was used for the gel filtration step. Based on the mobility shift by electrophoresis and in agreement with the literature, we confirmed that >75% of the *E. coli*–purified mArf1p, either wild-type or the dominant-activated mutant, was *N*-myristoylated. The purification resulted in ∼80% pure mArf1p.

The Chs5p–Chs6p complex was purified using the Bac-to-Bac baculovirus expression system (Invitrogen). To make the recombinant viruses for the baculovirus expression system, we used pFastBac (Invitrogen) to clone all Chs6p-like proteins, and pFastBac-HT was used to clone Chs5p, resulting in an N-terminal 6× His tag. Genes were cloned independently into constructs followed by transformation into DH10Bac competent cells for the production of recombinant bacmid vectors. Bacmid DNA was then transfected into Sf-9 insect cells, and viruses were amplified separately and kept frozen at −80°C for later use; the same virus stocks were thawed from a small aliquot, and the virus titer remained constant. 500 ml of insect cultures (Sf-9) were infected with the indicated virus stock; for example, 500 μl of virus stock of His-Chs5, Chs6, Bch1, Bund7, and Bch2 was added, respectively, into the same culture to assemble the Chs5–Chs6[all] complex. Infected cultures were harvested after 4 d of growth at room temperature.

Cells were lysed in 20 ml of lysis buffer I (50 mM Hepes, pH 7.4, 450 mM KOAc, 0.1 mM EGTA, 20 mM imidazole, and 10% glycerol) supplemented with 1× protease inhibitor cocktail and 1 mM PMSF. The lysate was centrifuged at 12,000 rpm for 10 min (SS34 rotor; Sorvall), and the resulting supernatant was incubated with 5 ml Ni–nitrilotriacetic acid (NTA) agarose at 4°C for 3–4 h. Beads were washed first with 20 ml of lysis buffer I followed by washing twice with wash buffer II (50 mM MES, pH 6.3, 450 mM KOAc, 0.1 mM EGTA, 40 mM imidazole, 10% glycerol, and 1 mM PMSF), three additional washes with wash buffer III (50 mM Hepes, pH 7.4, 450 mM KOAc, 250 mM sorbitol, 0.1 mM EGTA, 40 mM imidazole, 10% glycerol, and 1 mM PMSF), and one wash with HKG (50 mM Hepes, pH 7.4, 50 mM KOAc, and 10% glycerol). Bound proteins were eluted with HKGI buffer (50 mM Hepes, pH 7.4, 50 mM KOAc, 10% glycerol, and 0.5 M imidazole), and the elution was then dialyzed against HKG with three changes of buffer. Precipitation occurred during dialysis, and the protein aggregates were removed by centrifugation at 14,000 rpm at 4°C for 5 min. The protocol results in a >90% pure protein complex at a protein concentration of ~0.5 mg/ml. If necessary, the complex was concentrated by loading a 1-ml aliquot of the Ni-NTA fraction on a 200-μl, 2.2 M sucrose cushion followed by 100,000 rpm centrifugation for 1.5 h (TLA100.3 rotor; Beckman Coulter). Most proteins were recovered in the sucrose fraction. This procedure yielded approximately >1 mg/ml of pure complex.

Arf1-PA pull-down experiment

CWY506 cells were harvested at A_{600} = ~1.0 from 100 ml of culture. Cells were lysed by agitation with glass beads in 2.5 ml of lysis buffer B88, 1× complete protease inhibitor cocktails, and 1 mM PMSF. Total cell lysates were centrifuged at 20,000 *g* for 10 min at 4°C. To the resulting supernatant, we added 0.5 mM of nucleotide where indicated and incubated at 30°C for 10 min. 20 μl IgG-coated Dynabeads were added and incubated at 4°C for 2 h. Procedures for IgG coating on Dynabeads were provided by the manufacturer. Dynabeads were recovered by binding to a magnet, and beads were washed with 1 ml B88 buffer three times. Bound proteins were eluted in 100 μl SDS-PAGE resuspension buffer, and 10 μl was loaded on SDS-PAGE followed by immunoblot analysis.

Liposome recruitment assay

Liposomes were prepared as described previously except 1 mol percentage of Texas red–PE was substituted for NBD phospholipids (Matsuoka et al., 1998; Spang et al., 1998). In brief, 2 mM of lipid mixtures based on the lipid composition indicated in Fig. 4 B were prepared, and the organic solvent was evaporated by a rotavapor. HK buffer (20 mM Hepes, pH 6.8, and 160 mM KOAc) was applied to dried lipids, and the suspension was incubated at room temperature overnight followed by 19 passages through a 400-nm Nuclepore polycarbonate membrane.

20 μl of liposomes consisting of ~1 mM of lipids were incubated for 1 h at 30°C with 1.9 μg of purified mArf1p (final concentration of ~1 μM in a 80-μl standard reaction) and 0.1 mM nucleotide (GDP, GTP, or GTPγS) in a buffer composed of ~20 mM Hepes, pH 7.4, 1.2 mM $MgCl_2$, 2.5 mM EDTA, 50 mM NaCl, and 15 mM KOAc. Samples were returned to ice, and 2 mM $MgCl_2$ was added to stabilize the nucleotide-loaded mArf1p. The reaction was then adjusted to 80 μl by the addition of 0.5 μM Chs5–Chs6[all] complex (mol wt of ~300 kD) or as indicated. In a second stage, complex recruitment was conducted in a buffer composed of ~38 mM Hepes, pH 7.4, 1 mM EDTA, 1.7 mM $MgCl_2$, 18.75 mM NaCl, 35 mM KOAc, and 6.25% glycerol and followed by the binding step at room temperature for 15 min unless otherwise indicated. Samples were then transferred to ice and mixed with 50 μl of 2.5 M sucrose in HKM buffer (20 mM Hepes, pH 6.8, 160 mM KOAc, and 1 mM $MgCl_2$). A 110-μl sample was removed to a tube (TLA-100; Beckman Coulter) and layered with 100 μl of 0.75 M sucrose in HKM and 20 μl HKM, sequentially. Samples were centrifuged in a TLA-100 rotor (Beckman Coulter) at 100,000 rpm for 25 min at 24°C. The upper 30-μl fractions were carefully removed after centrifugation, 5 μl of which was used for the determination of lipid recovery based on the fluorescence of Texas red–PE. The remaining floated fraction (20 μl) was resuspend in SDS-PAGE resuspension buffer, and the amount applied to SDS-PAGE was based on lipid recovery. Gels were stained with Sypro red, images were taken using a Typhoon imager (GE Healthcare), and quantification was performed using ImageQuant software (GE Healthcare).

Gel filtration and gradient analysis

The gel filtration experiment was performed using an AKTA FPLC system (GE Healthcare). The mol wt standards for this experiment contained 1 mg/ml blue dextran (2,000 kD), 2.5 mg/ml thyroglobulin (669 kD), 0.15 mg/ml ferritin (440 kD), 1 mg/ml catalase (232 kD), 1 mg/ml aldolase (158 kD), 4 mg/ml BSA (74 kD), 0.15 mg/ml ribonuclease (13.7 kD), and 1 mg/ml cytochrome C (12.4 kD). 200-μl samples (~0.5–1.0 mg/ml) of a purified complex were injected into the system using a constant flow rate at 0.2 ml/min and collected into fractions of 250 μl. A 10-μl aliquot of each fraction was analyzed by SDS-PAGE followed by Sypro red staining. Quantification was performed using a Typhoon imager and ImageQuant software. To check the integrity of the purified Chs5–Chs6[all] complex, we performed a sucrose velocity gradient analysis. A 120-μl sample containing ~60 μg of purified complex was loaded on top of a 1.89-ml 10–50% linear sucrose gradient in HKM, and centrifugation was performed for 16 h at 4°C in a rotor (TLS55; Beckman Coulter) at 55,000 rpm. Similar gradient conditions were used to check lipid and protein distribution in the standard incubation, and 160 μl of the reaction mixture was applied instead. A total of 20 fractions (20 × 100 μl) were collected from the top of this gradient, and the sucrose concentration was determined using a refractometer (Fisher Scientific). To check lipid recovery, we removed a 50-μl sample from each fraction into a microtiter plate for quantification of the fluorescence of the Texas red–PE. SDS-PAGE resuspension buffer was added to the remaining fraction, and proteins were analyzed by SDS-PAGE and Sypro red staining. Quantification was performed using a Typhoon imager and ImageQuant software.

Fluorescence and electron microscopy

All strains used for microscopy were grown in synthetic dextrose (SD) medium to mid-log phase. Cells were incubated either at 26°C or shifted to 37°C for 40 min before examination. Microscopy was performed using a fluorescence microscope (Eclipse E600; Nikon). Images were captured by a CCD camera (C4742-95; Hamamatsu) using Image-Pro software (Media Cybernetics). For thin section microscopy, we fixed a standard reaction as described in the Liposome recruitment assay section with 2% glutaldehyde and 1% osmium tetroxide in cacodylate buffer for 1 h on ice. Samples were centrifuged using a TLA100.3 rotor (Beckman Coulter) at 55,000 rpm for 30 min. Membrane pellet fractions were processed for thin section electron microscopy as described previously (Orci et al., 1993).

Online supplemental material

Fig. S1 shows that Chs5p colocalized with Sec7p to the late Golgi compartment. Although the Chs5p-GFP/RFP signal was diffusely distributed at the restrictive temperature in the *sec7-4* strain, other Golgi marker signals were focused and more exaggerated, indicating that the Golgi membrane did not disperse in the *sec7-4* strain. Online supplemental material is available at http://www.jcb.org/cgi/content/full/jcb.200605106/DC1.

We thank Drs. Eugene Futai, Jinoh Kim, and other members of the Schekman laboratory for discussion and encouragement and Bob Lesch and Crystal Chan for technical assistance. We thank Pierre Cosson for the suggestion of the name exomer as well as for improving the manuscript. We are grateful to have had Drs. Robyn Barfield, Alenka Copic, Jinoh Kim, and Trevor Starr improve the manuscript. We thank Drs. David Drubin and Georjana Barnes for use of their FPLC system and microscope, Jasper Rine for access to his fluorescence microscope, Jeremy Thorner for the *pik1-83* strain, and Ann Fischer for the cell culture facility. We thank the Pole Facultaire de Microscopie Ultrastructure at the University of Geneva Medical School for access to electron microscopy equipment.

This work was supported by the National Institutes of Health (grant GM26755), the Howard Hughes Medical Institute (grant to R. Schekman), and the Swiss National Science Foundation (grant to L. Orci).

Submitted: 16 May 2006
Accepted: 18 August 2006

References

Ang, A.L., T. Taguchi, S. Francis, H. Folsch, L.J. Murrells, M. Pypaert, G. Warren, and I. Mellman. 2004. Recycling endosomes can serve as intermediates during transport from the Golgi to the plasma membrane of MDCK cells. *J. Cell Biol.* 167:531–543.

Antonny, B., S. Beraud-Fufour, P. Chardin, and M. Chabre. 1997. N-terminal hydrophobic residues of the G-protein ADP-ribosylation factor-1 insert into membrane phospholipids upon GDP to GTP exchange. *Biochemistry.* 36:4675–4684.

Antonny, B., P. Gounon, R. Schekman, and L. Orci. 2003. Self-assembly of minimal COPII cages. *EMBO Rep.* 4:419–424.

Audhya, A., M. Foti, and S.D. Emr. 2000. Distinct roles for the yeast phosphatidylinositol 4-kinases, Stt4p and Pik1p, in secretion, cell growth, and organelle membrane dynamics. *Mol. Biol. Cell*. 11:2673–2689.

Barlowe, C., L. Orci, T. Yeung, M. Hosobuchi, S. Hamamoto, N. Salama, M.F. Rexach, M. Ravazzola, M. Amherdt, and R. Schekman. 1994. COPII: a membrane coat formed by Sec proteins that drive vesicle budding from the endoplasmic reticulum. *Cell*. 77:895–907.

Bednarek, S.Y., L. Orci, and R. Schekman. 1996. Traffic COPs and the formation of vesicle coats. *Trends Cell Biol.* 6:468–473.

Deitz, S.B., A. Rambourg, F. Kepes, and A. Franzusoff. 2000. Sec7p directs the transitions required for yeast Golgi biogenesis. *Traffic*. 1:172–183.

Donaldson, J.G., D. Finazzi, and R.D. Klausner. 1992. Brefeldin A inhibits Golgi membrane-catalysed exchange of guanine nucleotide onto ARF protein. *Nature*. 360:350–352.

Flanagan, C.A., E.A. Schnieders, A.W. Emerick, R. Kunisawa, A. Admon, and J. Thorner. 1993. Phosphatidylinositol 4-kinase: gene structure and requirement for yeast cell viability. *Science*. 262:1444–1448.

Godi, A., A. Di Campli, A. Konstantakopoulos, G. Di Tullio, D.R. Alessi, G.S. Kular, T. Daniele, P. Marra, J.M. Lucocq, and M.A. De Matteis. 2004. FAPPs control Golgi-to-cell-surface membrane traffic by binding to ARF and PtdIns(4)P. *Nat. Cell Biol.* 6:393–404.

Hama, H., E.A. Schnieders, J. Thorner, J.Y. Takemoto, and D.B. DeWald. 1999. Direct involvement of phosphatidylinositol 4-phosphate in secretion in the yeast *Saccharomyces cerevisiae*. *J. Biol. Chem.* 274:34294–34300.

Kaksonen, M., Y. Sun, and D.G. Drubin. 2003. A pathway for association of receptors, adaptors, and actin during endocytic internalization. *Cell*. 115:475–487.

Kaksonen, M., C.P. Toret, and D.G. Drubin. 2005. A modular design for the clathrin- and actin-mediated endocytosis machinery. *Cell*. 123:305–320.

Le Borgne, R., and B. Hoflack. 1998a. Mechanisms of protein sorting and coat assembly: insights from the clathrin-coated vesicle pathway. *Curr. Opin. Cell Biol.* 10:499–503.

Le Borgne, R., and B. Hoflack. 1998b. Protein transport from the secretory to the endocytic pathway in mammalian cells. *Biochim. Biophys. Acta*. 1404:195–209.

Lee, M.C., E.A. Miller, J. Goldberg, L. Orci, and R. Schekman. 2004. Bi-directional protein transport between the ER and Golgi. *Annu. Rev. Cell Dev. Biol.* 20:87–123.

Lesage, G., J. Shapiro, C.A. Specht, A.M. Sdicu, P. Menard, S. Hussein, A.H. Tong, C. Boone, and H. Bussey. 2005. An interactional network of genes involved in chitin synthesis in *Saccharomyces cerevisiae*. *BMC Genet.* 6:8.

Liljedahl, M., Y. Maeda, A. Colanzi, I. Ayala, J. Van Lint, and V. Malhotra. 2001. Protein kinase D regulates the fission of cell surface destined transport carriers from the trans-Golgi network. *Cell*. 104:409–420.

Longtine, M.S., A. McKenzie III, D.J. Demarini, N.G. Shah, A. Wach, A. Brachat, P. Philippsen, and J.R. Pringle. 1998. Additional modules for versatile and economical PCR-based gene deletion and modification in *Saccharomyces cerevisiae*. *Yeast*. 14:953–961.

Matsuoka, K., L. Orci, M. Amherdt, S.Y. Bednarek, S. Hamamoto, R. Schekman, and T. Yeung. 1998. COPII-coated vesicle formation reconstituted with purified coat proteins and chemically defined liposomes. *Cell*. 93:263–275.

Novick, P., C. Field, and R. Schekman. 1980. Identification of 23 complementation groups required for post-translational events in the yeast secretory pathway. *Cell*. 21:205–215.

Orci, L., D.J. Palmer, M. Ravazzola, A. Perrelet, M. Amherdt, and J.E. Rothman. 1993. Budding from Golgi membranes requires the coatomer complex of non-clathrin coat proteins. *Nature*. 362:648–652.

Orci, L., M. Stamnes, M. Ravazzola, M. Amherdt, A. Perrelet, T.H. Sollner, and J.E. Rothman. 1997. Bidirectional transport by distinct populations of COPI-coated vesicles. *Cell*. 90:335–349.

Palmer, D.J., J.B. Helms, C.J. Beckers, L. Orci, and J.E. Rothman. 1993. Binding of coatomer to Golgi membranes requires ADP-ribosylation factor. *J. Biol. Chem.* 268:12083–12089.

Randazzo, P.A., O. Weiss, and R.A. Kahn. 1992. Preparation of recombinant ADP-ribosylation factor. *Methods Enzymol.* 219:362–369.

Robinson, M.S. 1994. The role of clathrin, adaptors and dynamin in endocytosis. *Curr. Opin. Cell Biol.* 6:538–544.

Rothman, J.E., and F.T. Wieland. 1996. Protein sorting by transport vesicles. *Science*. 272:227–234.

Sanchatjate, S., and R. Schekman. 2006. Chs5/6 complex: a multi-protein complex that interacts with and conveys chitin synthase III from the trans-Golgi network to the cell surface. *Mol. Biol. Cell*. doi:10.1091/mbc.E06-03-0210.

Santos, B., and M. Snyder. 2000. Sbe2p and sbe22p, two homologous Golgi proteins involved in yeast cell wall formation. *Mol. Biol. Cell*. 11:435–452.

Santos, B., and M. Snyder. 2003. Specific protein targeting during cell differentiation: polarized localization of Fus1p during mating depends on Chs5p in *Saccharomyces cerevisiae*. *Eukaryot. Cell*. 2:821–825.

Santos, B., A. Duran, and M.H. Valdivieso. 1997. CHS5, a gene involved in chitin synthesis and mating in *Saccharomyces cerevisiae*. *Mol. Cell. Biol.* 17:2485–2496.

Schekman, R., and L. Orci. 1996. Coat proteins and vesicle budding. *Science*. 271:1526–1533.

Serafini, T., G. Stenbeck, A. Brecht, F. Lottspeich, L. Orci, J.E. Rothman, and F.T. Wieland. 1991. A coat subunit of Golgi-derived non-clathrin-coated vesicles with homology to the clathrin-coated vesicle coat protein beta-adaptin. *Nature*. 349:215–220.

Shaw, J.A., P.C. Mol, B. Bowers, S.J. Silverman, M.H. Valdivieso, A. Duran, and E. Cabib. 1991. The function of chitin synthases 2 and 3 in the *Saccharomyces cerevisiae* cell cycle. *J. Cell Biol.* 114:111–123.

Shimoni, Y., T. Kurihara, M. Ravazzola, M. Amherdt, L. Orci, and R. Schekman. 2000. Lst1p and Sec24p cooperate in sorting of the plasma membrane ATPase into COPII vesicles in *Saccharomyces cerevisiae*. *J. Cell Biol.* 151:973–984.

Simon, J.P., I.E. Ivanove, M. Adesnik, and D.D. Sabatini. 1996. The production of post-Golgi vesicles requires a protein kinase C-like molecule, but not its phosphorylating activity. *J. Cell Biol.* 135:355–370.

Spang, A., and R. Schekman. 1998. Reconstitution of retrograde transport from the Golgi to the ER in vitro. *J. Cell Biol.* 143:589–599.

Spang, A., K. Matsuoka, S. Hamamoto, R. Schekman, and L. Orci. 1998. Coatomer, Arf1p, and nucleotide are required to bud coat protein complex I-coated vesicles from large synthetic liposomes. *Proc. Natl. Acad. Sci. USA*. 95:11199–11204.

Springer, S., and R. Schekman. 1998. Nucleation of COPII vesicular coat complex by endoplasmic reticulum to Golgi vesicle SNAREs. *Science*. 281:698–700.

Strahl, T., H. Hama, D.B. DeWald, and J. Thorner. 2005. Yeast phosphatidylinositol 4-kinase, Pik1, has essential roles at the Golgi and in the nucleus. *J. Cell Biol.* 171:967–979.

Tong, A.H., G. Lesage, G.D. Bader, H. Ding, H. Xu, X. Xin, J. Young, G.F. Berriz, R.L. Brost, M. Chang, et al. 2004. Global mapping of the yeast genetic interaction network. *Science*. 303:808–813.

Trautwein, M., C. Schindler, R. Gauss, J. Dengjel, E. Hartmann, and A. Spang. 2006. Arf1p, Chs5p and the ChAPs are required for export of specialized cargo from the Golgi. *EMBO J.* 25:943–954.

Valdivia, R.H., and R. Schekman. 2003. The yeasts Rho1p and Pkc1p regulate the transport of chitin synthase III (Chs3p) from internal stores to the plasma membrane. *Proc. Natl. Acad. Sci. USA*. 100:10287–10292.

Valdivia, R.H., D. Baggott, J.S. Chuang, and R.W. Schekman. 2002. The yeast clathrin adaptor protein complex 1 is required for the efficient retention of a subset of late Golgi membrane proteins. *Dev. Cell*. 2:283–294.

Walch-Solimena, C., and P. Novick. 1999. The yeast phosphatidylinositol-4-OH kinase pik1 regulates secretion at the Golgi. *Nat. Cell Biol.* 1:523–525.

Ziman, M., J.S. Chuang, M. Tsung, S. Hamamoto, and R. Schekman. 1998. Chs6p-dependent anterograde transport of Chs3p from the chitosome to the plasma membrane in *Saccharomyces cerevisiae*. *Mol. Biol. Cell*. 9:1565–1576.